Digest Journal of Nanomaterials and Biostructures Vol. 19, No. 3, July -September 2024, p. 1243 - 1253

The effect of uniaxial mechanical stress on electronic and dynamic properties of silicon

R. Aliev[a], B. Rashidov[a], A. Mirzaalimov[b], N. Mirzaalimov[a], S. Aliev[c], I. Gulomova[a,*], J. Gulomov[b]
[a]*Andijan State University, Andijan, 170100, Uzbekistan*
[b]*Andijan State Pedagogical Institute, Andijan, 170100, Uzbekistan*
[c]*Andijan Machine Building Institute, Andijan, 170119, Uzbekistan*

This study explores the variation of highly symmetric points in the band structure, revealing a shift from G-X symmetric K path to Z-G path under the influence of mechanical stress. Notably, the band gap decreased linearly with increasing mechanical stress, while the effective mass of the electron, heavy hole, and light hole exhibited different trends. The variation of band gap, effective mass of electron, heavy and light holes, electron affinity, dielectric constant in x and y direction has been found to be -0.1238 eV/GPa, -6E-3 1/GPa, -7.9E-3 1/GPa, 1.4E-2 1/GPa, 4.7e-2 eV/GPa, 7.3e-2 1/GPa and -10.3e-2 1/GPa, respectively.

(Received April 20, 2024; Accepted August 14, 2024)

Keywords: DFT, Silicon, Effective mass, Mechanical stress, Phonon dispersion

1. Introduction

Silicon, the one of the important materials of our modern world. Notably, 90% of industrial solar cells are produced from silicon [1]. However, the cost reduction and efficiency enhancement of these solar cells remains a significant task. According to the Shockley-Quisser theory, the maximum efficiency of silicon-based solar cells is the 29% mark [2] and in laboratory, efficiency has been recorded at to 27.6% [3]. Various factors contribute to this limitation, including thermal, electrical, and optical losses within the solar cell [4]. Front surface of solar cells is covered with anti-reflection coatings to minimize the reflection of incident light [5]. Electrical losses, on the other hand occur due to recombination and the presence of both series and parallel resistances [6]. Strategies involving the use of passivating materials have been implemented to mitigate surface recombination and improve overall performance of solar cell. SiO_2 [7] and SiN_x [8], known for their anti-reflection and passivation properties, are commonly utilized as coatings for silicon-based solar cells. Another critical factor influencing the efficiency of these solar cells is temperature [9]. As the temperature rises, the efficiency of silicon-based solar cells tends to decrease. Industrial solar cells, with their flat back contacts, have a tendency to absorb infrared rays, leading to elevated temperatures within the cell [10]. To overcome this challenge, a grid view design has been adopted for the rear contact, effectively reducing heat buildup and enhancing the cell's performance.

To enhance the light absorption spectrum of silicon-based solar cells, coating their surface with luminescent materials [11] or introducing metal nanoparticles [12] has emerged as a promising approach. These techniques aim to expand the range of wavelengths that can be captured, improving the efficiency and performance of the solar cells.

In conventional solar cells featuring a p-n junction, the generation of photocurrent and photovoltage is mainly due to the photovoltaic effect. According to the researches of recent years [13], photovoltage and photocurrent are also generated when a local mechanical force is applied to a semiconductor crystal and it is illuminated at the same time. Because an internal electric field is created due to the formation of a gradient stress in the crystal, which helps to separate the excitons generated in the photogeneration and reach them to electrodes. The gradient stress acts as a p-n junction. This phenomenon is called flexophotovoltaic effect. While numerous scientific studies

[*] Corresponding author: irodakhon.gulomova@yahoo.com
https://doi.org/10.15251/DJNB.2024.193.1243

have investigated the impact of mechanical force on illuminated silicon crystals and unilluminated silicon p-n junctions, the influence of mechanical force on an illuminated silicon p-n junction remains a relatively underexplored area in research. Therefore, in our previous exploration, we conducted experimental studies to explore the impact of local mechanical stress on silicon-based p-n junction solar cells [14]. The results revealed an increase in the short-circuit current and a decrease in the open circuit voltage of the monocrystalline silicon-based solar cell. Since mechanical stress directly influences material properties, subjecting the solar cell to such stress leads to alterations in its output parameters. Under mechanical stress indirect-to-direct bandgap transition can be observed [15]. Silicon has a cubic symmetrical crystal. But when a mechanical stress is applied to it in one direction, its crystal lattice changes from a cubic to a triclinic structure. Because, when a mechanical force is applied to the crystal lattice on one side, it is compressed in the direction of the force, but it expands on the other two sides. When there is no external influence, the atoms in the crystal lattice are placed in their most optimal position, where the total energy of the crystal is minimal. When the crystal is subjected to an external mechanical stress, the arrangement of atoms changes according to a certain law to compensate the mechanical stress energy and maintain the crystal stability. Because the interaction between atoms depends on the arrangement of atoms. Understanding the scientific basis for these changes and unraveling the underlying mechanisms within the solar cell under mechanical stress is of paramount importance. To address this scientific gap and gain insights into the behavior of monocrystalline silicon subjected to mechanical stress in the (100) direction, we undertook a study employing Density Functional Theory (DFT). By utilizing this theoretical approach, we aimed to comprehensively investigate the effect of mechanical stress on the material properties of monocrystalline silicon. The findings from this research contribute to the broader understanding of the flexophotovoltaic effect and offer valuable insights into harnessing mechanical stress as a means to enhance the performance of silicon-based solar cells.

This article is composed of four sections: an Introduction presenting the context and objectives, a Materials and Methods section detailing the simulation process and approach, a Results and Discussion section, which interprets and contextualizes the findings, and finally, a Conclusion that summarizes the key insights and potential implications of the study.

2. Materials and method

Necessary physical parameters of mechanical stress applied monocrystalline silicon was calculated using the first-principles method with the CASTEP [16] code. The first-principles method is to calculate the physical properties of the material directly using initial physical values, such as mass-charge and electron interactions, using the Schrodinger equation, making several approximations. As an approximation in the first principles method, Harte-Fock (HF) theory [17] and Density functional theory (DFT) [18] is used. HF mainly approximates the wave function as the Slater determinant [19], while DFT formulates the many-body system as the electron density and derives from the Khon-Sham equation given formula 1 [20] finds the main state characteristics of the system.

$$\left[-\frac{\nabla^2}{2m^*}+v_{ext}(r)+v_H(r)+v_{XC}(r)\right]\phi_n(r)=\varepsilon_n\phi_n(r) \tag{1}$$

Here: m^* is effective mass, v_{ext} is extrenal potential, v_H is Hartree potential, v_{XC} is exchange-correlation potential, ε_n is eigenvalues and ϕ_n is Khon-sham wavefunction.

In this work, DFT was employed to model monocrystalline silicon. The calculation of the electron exchange-correlation energy utilized the local density approximation (LDA) [21], generalized gradient approximation (GGA) [22] and hybrid functionals (XC) [23]. The Perdew-Burke-Ernzerhof (PBE) functionals of GGA [24] and HSE06 [25] of XC are widely used for calculating the electronic properties of crystals. While PBE functional offers fast but less precise results when calculating the band structure, the HSE06 functional requires extensive computational time but delivers highly accurate results. Given its high accuracy, the HSE06 was chosen to compute the exchange-correlation energy of electrons.

In material simulation, the geometry optimization is performed to determine the optimal arrangement of atoms in the crystal to establish the minimum total energy of the structure before calculating the electrical and optical properties. When a mechanical stress is applied to a crystal, the arrangement of atoms changes to counteract the external mechanical stress. A mechanical stress from 0 GPa to 6 GPa was incrementally applied to the silicon crystal in 1 GPa step according to the flowchart shown in figure 1.

After each mechanical force application, the structure was geometrically reoptimized using the Broyden–Fletcher–Goldfarb–Shanno (BFGS) [26] algorithm to determine the optimal position of the atoms within the stress-applied. In CASTEP, as a basis set, the cut-off energy is used and it is set to 517 eV in this calculation. The calculation accuracies of the energy, displacement, interaction force, and mechanical stress in geometric optimization are 1.38e-5 eV/atom, 9.1e-6 A, 4.37e-4 eV/A, and 2.82e-3 GPa, respectively. The calculation of the band structure was carried out according to the Monkhorst-Pack max integration scheme with a 5x5x5 k-point grid. The accuracy of the energy and k-point difference in the calculation of the band structure was assumed to be 1e-6 eV/atom and 0.015 1/A, respectively. The interaction between the valence electron and the nucleus was determined by on-the-fly generation (OTFG) ultrasoft pseudopotential. The effective mass of charge carriers was determined by the parabolic curvature function of the band structure given formula 2. The parabolic approximation of the band structure was used to calculate the effective mass.

$$E(k) = E_0 + \frac{\hbar^2 k^2}{2m^*} \tag{2}$$

Here: E is the energy, E_0 is the energy at $k = 0$, k is the wavenumber, m^* is the effective mass, and $\hbar$ is the Planck constant.

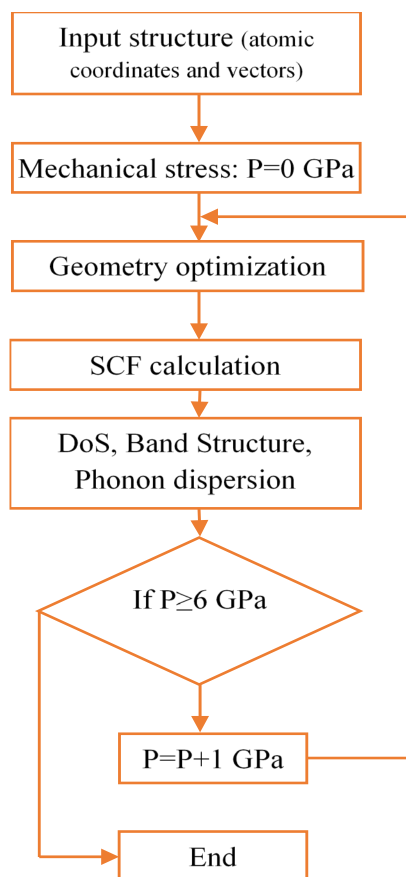

Fig. 1. Flowchart of simulation of mechanical stress applied silicon.

3. Results and discussion

3.1 Lattice parameters

Therefore, when the mechanical force is applied, it necessitates the geometric optimization of the crystal. Each change in the mechanical stress prompts a re-optimization of the crystal's geometry. Because, with the help of geometric optimization, it is possible to determine a mechanically stable crystal structure under a specific mechanical stress. In this scientific work, we applied mechanical stress to silicon in the (100) direction ranging from 1 GPa to 6 GPa. Figure 2 shows the dependence of the length and size of the sides of the crystal lattice of silicon on mechanical stress. Since the mechanical force is applied in the (100) direction, the length of the crystal is shortened. Also, the lengths of sides b and c are equally extended. The shape of the silicon crystal changed from cubic to tetragonal after applying mechanical force. Therefore, the connection between its sides is like a≠b=c. The change of the length of the a side of the crystal depending on the mechanical stress was -4.54e-2 A/GPa, and the change of the b side was equal to 1.36e-2 A/GPa. Since the degree of shortening of side a is greater than the that of expansion of sides b and c, the size of the crystal decreased under the influence of mechanical force. The reduction of the crystal volume depending on the mechanical stress was equal to -0.579 A^3/GPa. After geometrical optimization of the structure without mechanical stress, the crystal size was equal to 5.47 A. In the experiment, the side length of the silicon crystal is equal to 5.43.

The main properties of a semiconductor are analyzed using a band structure. Figure 3 depicts the band structure and density of states calculated using the HSE06 and PBE functionals of mechanically unstressed silicon. The quality of the band structure lines in HSE06 and PBE is almost the same. However, the band structure lines calculated in PBE were found to be closer to parallel to 0 eV compared to HSE06. The density of states calculated in PBE was also closer to 0 eV but almost identical to the line quality of the density of states calculated in HSE06. Nevertheless, the maximum points of density of states were higher in HSE06. Since the quality of the band structure and density of states lines calculated using both functionals is almost the same, the optimal functional can be determined depending on the value of the band gap.

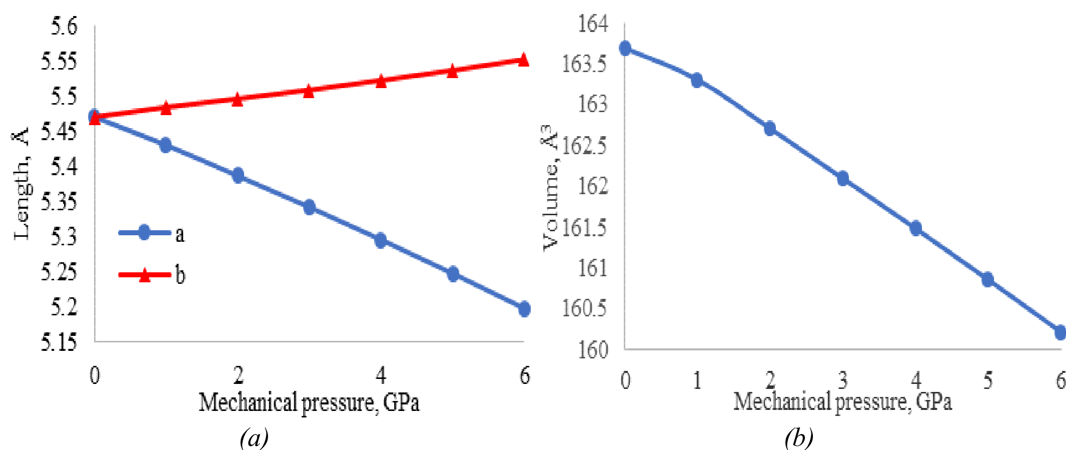

Fig. 2. Dependence of lengths (a) and volume (b) of crystal of silicon on mechanical stress.

3.2. Band structure

In the experiment, the band gap of silicon is equal to 1.12 eV. After the geometrical optimization of the structure, the band gap calculated by HSE06 and PBE was equal to 1.196 eV and 0.619 eV. The accuracy of HSE06 and PBE functionals in calculating the band gap of silicon was 94% and 55.3%. It was found that the band gap of the silicon crystal structure determined in the experiment is equal to 1.164 eV when the energy calculation is performed directly in HSE06 without geometric optimization. So, if the structure is not geometric optimized, the accuracy of HSE06 is equal to 96%. However, the application of a mechanical force to the structure leads to changes in the atomic positions, requiring geometric optimization to locate the optimal arrangement of atoms.

Also, the physical parameters of the structure determined when mechanical stress is applied cannot be directly compared with the physical parameters of the structure without geometric optimization and mechanical stress.

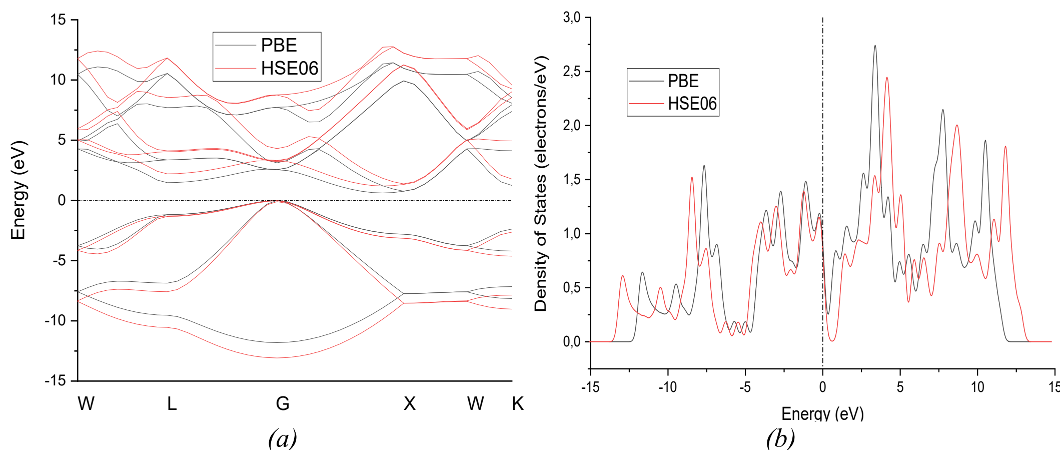

(a) *(b)*

Fig. 3. Band structure (a) and density of states (b) calculated in HSE06 and PBE of mechanically unstressed silicon.

In order to determine the general law of the effect of mechanical stress on silicon, the band gap of the geometrically optimized structure, i.e. 1.196 eV, was taken as the bandgap of the mechanically unstressed structure.The shift in the high symmetric points of the crystal was determined at the exact value of the mechanical stress. As the mechanical stress increased above 2 GPa, the band structure changed from highly symmetric points and paths (W-L-G-X-W-K) to (Z-G-X-P-N-G). Therefore, Figure 4.a shows the band structure of silicon with mechanical stress of 0 GPa and 1 GPa, and Figure 4.b with mechanical stress of 2 GPa and 6 GPa. Upon the application of 1 GPa mechanical stress to silicon, the minimum point of the conduction zone did not shift along the k-axis, but moved toward 0 eV along the energy axis.

Even when the amount of mechanical stress increased from 2 GPa to 6 GPa, the minimum energy of the conduction zone did not shift along the k-axis. Therefore, when a mechanical force was applied to silicon, the minimum point of the conduction zone changed from the G-X symmetric K path to the Z-G path. Mechanical stress applied to silicon led to a decrease in its band gap due to lattice deformation, band splitting, quantum confinement effects, dielectric screening changes, and shifts in band extrema.

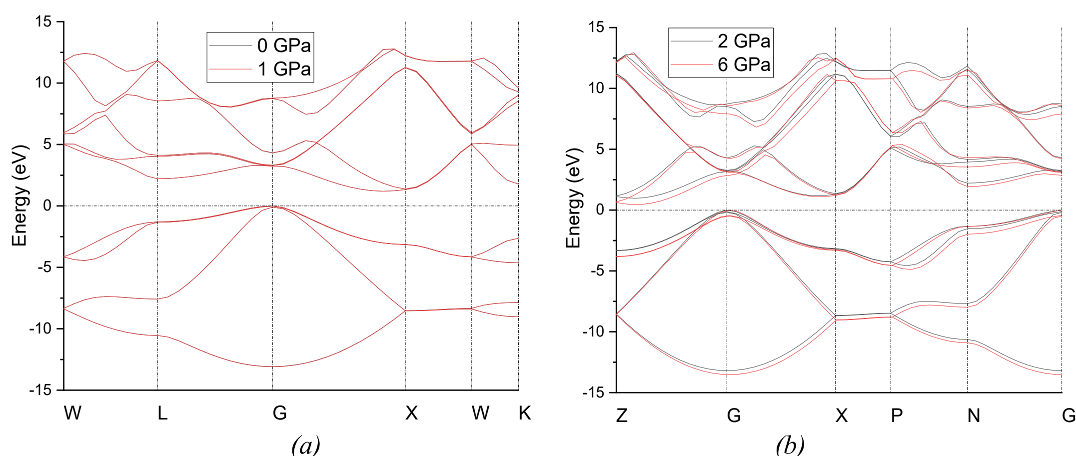

(a) *(b)*

Fig. 4. Band structure of silicon applied mechanical stress of 0 GPa, 1 GPa (a), 2 GPa and 6 GPa (b).

3.3. Phonon dispersion

Mechanical stability can be found by using stiffness matrix elements. But, to identify thermodynamic stability, phonon dispersion is widely used. Mechanical stress applied to a material leads to a distortion of its crystal lattice. This distortion affects the interatomic forces and alters the equilibrium positions of atoms within the lattice. The distortion of the lattice changes the force constants governing the interactions between atoms. These changes in force constants modify the vibrational frequencies of atoms around their equilibrium positions. We also calculated phonon dispersion of silicon unstressed and stressed. Figure 5 shows that phonon dispersion of silicon unstressed and stressed with 1 GPa. When we apply stress to silicon, atoms move in direction of stress. So, it effects on its stability and vibration of atoms. There are mainly two types of phonons: optic and acoustic. Phonons with higher frequency are called optic and lower ones are acoustic. According to figure 5, when mechanical stress applied to silicon, mainly frequency of acoustic phonons is increased. Longitudinal optic (LO) phonons didn't change but transverse optic (TO) phonons frequency increased. In acoustic mode, both of longitudinal acoustic (LA) and transverse acoustic (TA) frequencies are increased when mechanical stress is applied. Especially, there is no imaginary frequencies in phonon dispersion, it means that after applying mechanical stress, our structure is still stable. Furthermore, the phonon dispersion analysis offers valuable information about the interaction between lattice vibrations and mechanical stress, providing insights into the material's elastic properties. The distinction between longitudinal and transverse phonon modes elucidates the anisotropic behavior of silicon under stress, contributing to our understanding of its mechanical response. Additionally, the observed changes in phonon frequencies can be attributed to the alteration of interatomic forces within the crystal lattice, reflecting the material's dynamic adaptation to external pressure.

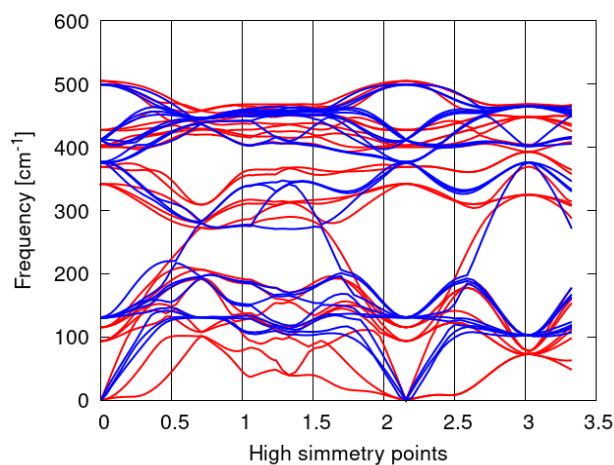

Fig. 5. Phonon dispersion of cubic silicon unstressed (red) and stressed (blue) with 1 GPa in (100) direction.

In Zileyvych's experiment [27], the band gap decreased linearly under the influence of mechanical force. In this scientific work, it was found that the quality of the dependence function of the band gap on the mechanical stress determined in HSE06 and PBE and depicted in Figure 6, is the same.

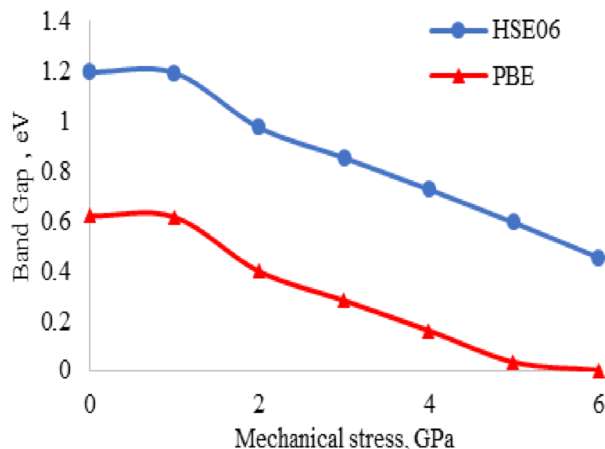

Fig. 6. Dependence of the band gap calculated in PBE and HSE06 on mechanical stress.

But the value of band gap calculated in HSE06 is closer to the experimental result. In the range of 2 GPa and 6 GPa mechanical stress, the band gap exhibited an almost linear shift, satisfying the expectations based on the experimental data. The variation of the band gap with respect to the mechanical stress was equal to 0.1238 eV/GPa.The effective mass shows the kinetic characteristics of the charge carriers in the semiconductor and the curvature of the band diagram. From the band structure, the effective mass can be determined using the parabolic approximation. The effective mass of the electron and the hole is determined by parabolic approximation of the E-k graph around the conduction band minimum and the valence band maximum. Figure 7 depicts the dependence of the effective mass of electron, heavy and light holes in silicon on mechanical stress.

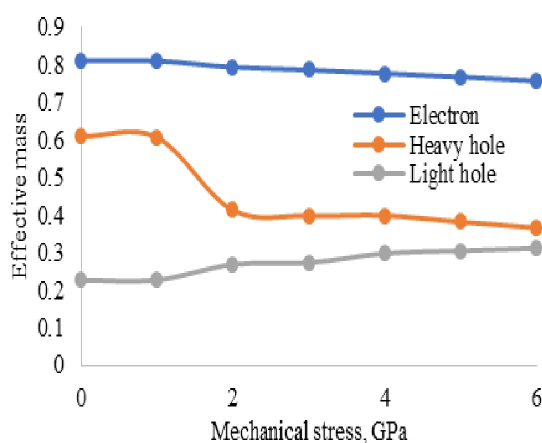

Fig. 7. Dependence of the effective mass of electron, heavy and light holes on mechanical stress.

The effective masses of electron, heavy and light holes in unstressed silicon calculated using the HSE06 functional were equal to 0.8114, 0.6088 and 0.2268, respectively. According to the experimental findings [28], their effective mass is 0.98, 0.49 and 0.16. The effective mass of the electron decreased linearly by the amount of 6E-3 1/GPa depending on the mechanical stress. Variation of the effective mass of the heavy hole depending on mechanical stress is -1.79E-3 1/GPa. When the mechanical stress changed from 1 GPa to 2 GPa, it decreased sharply by 0.194. In the range of mechanical stress from 2 GPa to 6 GPa, it decreased linearly by the amount of 7.9E-3 1/GPa depending on the mechanical stress. As the highly symmetric points in the band structure of silicon jump when the mechanical stress changes from 1 GPa to 2 GPa, the effective mass of the heavy hole also changes dramatically. The effective mass of the light hole increased almost linearly under

mechanical stress. The variation of the effective mass of the light hole depending on mechanical stress was equal to 1.4E-2 1/GPa. When mechanical stress is applied, the curvature of the valence band may increase in certain directions, leading to increase of effective mass of light holes due to stronger confinement. Therefore, the decrease in the effective mass of the electron and heavy hole when mechanical stress is applied can be attributed to weaker confinement. Changing of the band structure cause the altering of the electron affinity. In figure 8 dependence of electron affinity on mechanical stress is show. When mechanical stress increase, band gap decrease but electron affinity increase almost linearly with coefficient of 4.7e-2 eV/GPa. It means that decreasing of band gap is due to mainly shifting down of conduction band minima. Mechanical stress alters the spacing between atoms in the crystal lattice, affecting the electronic band structure. In silicon, compressive stress can increase the overlap between the valence and conduction bands, effectively reducing the band gap. This reduction in band gap makes it easier for electrons to move from the valence band to the conduction band, thus increasing the electron affinity.

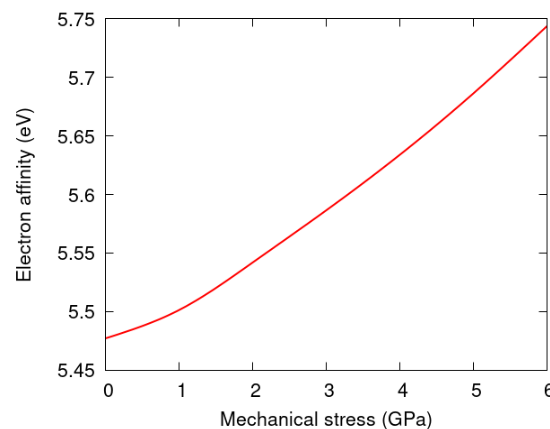

Fig. 8. Dependence of electron affinity (b) of stressed silicon on mechanical stress.

The dielectric constant, also known as relative permittivity, is a measure of how easily a material can be polarized by an electric field. In semiconductors, this property affects their ability to store electrical energy when subjected to an electric field. In figure 9, dependence of dielectric constant on mechanical stress is shown. Because of mechanical stress is applied in x direction, dielectric constant in that direction is decreased with coefficient of -10.3e-2 1/GPa but in y and z direction increased with coefficient of 7.3e-2 1/GPa. In Unruan's work [29], it was found that dielectric constant of the materials increases when mechanical stress is applied.

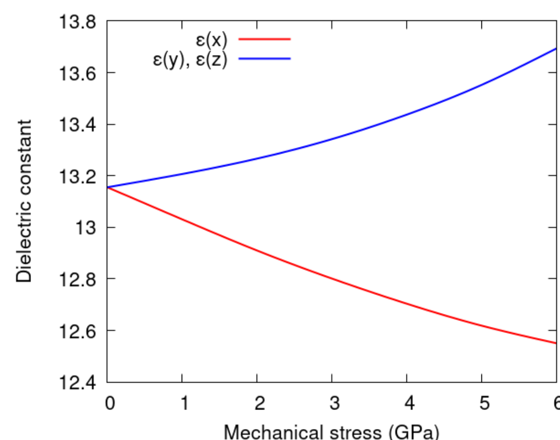

Fig. 9. Dependence of dielectric constant of silicon on mechanical stress.

Our structure was cubic, so unstressed silicon has the same dielectric constant in all direction. After applying mechanical stress, length of a in X direction is decreased and length of b and c are increased. So, dielectric constant is proportional to lattice constant. Mechanical stress can indeed affect the mobility of charge carriers in silicon. This effect is commonly known as piezo-resistance. When mechanical stress is applied to a silicon crystal lattice, it can alter the spacing between atoms, modifying the energy bands and affecting the mobility of charge carriers within the material. In figure 10, dependence of electron and hole mobility on mechanical stress is shown. When mechanical stress increase, mobility of electron and holes decrease. It is observed that mobility of holes increased when mechanical stress changed from 0 GPa to 2 GPa. In between 2-6 GPa mechanical stress, mobility of hole and electrons are changed linearly. Charge carriers in a material can interact with lattice vibrations (phonons) through various scattering mechanisms, such as deformation potential scattering and electron-phonon coupling.

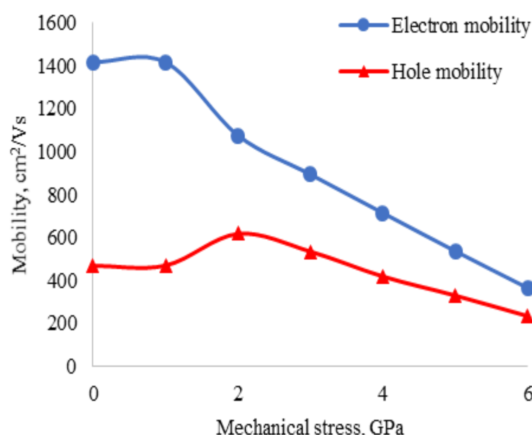

Fig. 10. Dependence of electron and hole mobilities of silicon on mechanical stress.

Higher frequency phonons, which result from mechanical stress, can lead to increased scattering of charge carriers. The increased scattering of charge carriers by high-frequency phonons effectively reduces their mobility in the material. As charge carriers move through the crystal lattice, they scatter off phonons, leading to a deviation from the ideal ballistic transport and a decrease in carrier mobility.

4. Conclusion

In conclusion, this study investigated the effects of mechanical stress on silicon. When subjected to mechanical force in the [100] direction, the crystal lattice of silicon changed resulting in a decrease in the length of side "a" and an expansion of sides "b" and "c," ultimately leading to an overall reduction in crystal volume. The effective mass of the electron and heavy hole exhibited a linear decrease with increasing mechanical stress. Simultaneously, the band gap of silicon decreased linearly with mechanical stress, indicating an increase in the concentration of intrinsic charge carriers.

These results have important implications for various applications. It would also lead to a decrease in open circuit voltage due to the narrowing of the band gap.

The findings of this research also shed light on the influence of mechanical stress on the band structure and effective mass. The band structure analysis revealed shifts in highly symmetric points as the mechanical stress increased, which was agree with previous experimental results. Additionally, the calculated band gap closely aligned with experimental data.

As a result, this study provides valuable insights into the behavior of silicon under mechanical stress, offering a basis for further research and potential applications in semiconductor devices and solar cell technologies. The observed relationships between mechanical stress, crystal lattice changes, and material properties contribute to a better understanding of the physical behavior of the effect of mechanical stress on silicon solar cell. In the future, we want to study the effect of local mechanical stress on silicon solar cells using properties of mechanical stressed silicon determined in this article.

Acknowledgments

We extend our sincere thanks to the team at the Renewable Energy Source Laboratory, Andijan State University, for their invaluable assistance in completing this work. Their expertise and support were instrumental in the success of our research endeavors.

References

[1] X. Wang, X. Tian, X. Chen, L. Ren, C. Geng, Solar Energy Materials and Solar Cells, 248, 111976 (2022); https://doi.org/10.1016/j.solmat.2022.111976

[2] B. Ehrler, E. Alarcón-Lladó, S. W. Tabernig, T. Veeken, E. C. Garnett, A. Polman, ACS Energy Letter, 5(9), 3029 (2020); https://doi.org/10.1021/acsenergylett.0c01790

[3] M. A. Green et al., Progress in Photovoltaics: Research and Applications, 30(7), 687 (2022); https://doi.org/10.1002/pip.3595

[4] J. Pastuszak, P. Węgierek, Materials, 15(16), 5542 (2022); https://doi.org/10.3390/ma15165542

[5] X. J. Xiao, H. M. Zhu, Z. M. Liu, J. L. Tu, Materwiss Werksttech, 53(1), 80 (2022); https://doi.org/10.1002/mawe.202100188

[6] Z. Sun et al., Advanced Energy Materials, 12(23), 2200015 (2022); https://doi.org/10.1002/aenm.202200113

[7] C. J. Ruud, A. Cleri, J. P. Maria, N. C. Giebink, Nano Letters, 22(18), 7358 (2022); https://doi.org/10.1021/acs.nanolett.2c01945

[8] A. Cordaro et al., physica status solidi (a), 220(5), 2200827 (2023); https://doi.org/10.1002/pssa.202200881

[9] A. A. Zaky, S. Elewa, S. Alyahya, M. Al-Dhaifallah, H. Rezk, B. Yousif, IEEE Access, 11, 36399 (2023); https://doi.org/10.1109/ACCESS.2023.3266240

[10] J. Kim et al., IEEE Access, 11, 21326 (2023); https://doi.org/10.1109/ACCESS.2023.3248795

[11] O. D. Miller, E. Yablonovitch, S. R. Kurtz, IEEE Journal of Photovoltaics, 2(3), 303 (2012); https://doi.org/10.1109/JPHOTOV.2012.2198434

[12] J. Gulomov, O. Accouche, IEEE Access, 10, 119558 (2022); https://doi.org/10.1109/ACCESS.2022.3221875

[13] M. M. Yang, D. J. Kim, M. Alexe, Science, 360(6391), 904 (2018); https://doi.org/10.1126/science.aan3256

[14] J. Gulomov, O. Accouche, B. Rashidov, Z. Al Barakeh, M. Azab, IEEE Access, 11, 82248 (2023); https://doi.org/10.1109/ACCESS.2023.3301129

[15] Z. Shi, E. Tsymbalov, M. Dao, S. Suresh, A. Shapeev, J. Li, Proceedings of the National Academy of Sciences of the United States of America, 116(10), 4117 (2019); https://doi.org/10.1073/pnas.1818555116

[16] M. D. Segall et al., Journal of Physics: Condensed Matter, 14(11), 2717 (2002); https://doi.org/10.1088/0953-8984/14/11/301

[17] C. Froese Fischer, Computer Physics Communications, 43(3), 355 (1987); https://doi.org/10.1016/0010-4655(87)90053-1

[18] J. Neugebauer, T. Hickel, Wiley Interdisciplinary Reviews: Computational Molecular Science, 3(5), 438 (2013); https://doi.org/10.1002/wcms.1125

[19] J. C. Slater, Physical Review, 34(10), 1293 (1929); https://doi.org/10.1103/PhysRev.34.1293

[20] V. Sahni, Quantal Density Functional Theory, 99 (2004); https://doi.org/10.1007/978-3-662-09624-6_4

[21] A. D. Becke, The Journal of Chemical Physics, 98(2), 1372 (1993); https://doi.org/10.1063/1.464304

[22] J. P. Perdew, W. Yue, Physical Review B, 33(12), 8800 (1986); https://doi.org/10.1103/PhysRevB.33.8800

[23] A. V. Krukau, O. A. Vydrov, A. F. Izmaylov, G. E. Scuseria, Journal of Chemical Physics, 125(22), (2006); https://doi.org/10.1063/1.2404663

[24] M. Ernzerhof, G. E. Scuseria, The Journal of Chemical Physics, 110(11), 5029 (1999); https://doi.org/10.1063/1.478401

[25] J. Heyd, G. E. Scuseria, M. Ernzerhof, The Journal of Chemical Physics, 118(18), 8207 (2003); https://doi.org/10.1063/1.1564060

[26] J. D. Head, M. C. Zerner, Chemical Physics Letters, 122(3), 264 (1985); https://doi.org/10.1016/0009-2614(85)80574-1

[27] M. O. Zylevich, P. V. Kucherniuk, Visnyk NTUU KPI Seriia - Radiotekhnika Radioaparatobuduvannia, 85, 60 (2021).

[28] Jasprit Singh, "Semiconductor Devices: Basic Principles", Wiley, 576 (2023).

[29] M. Unruan, A. Prasatkhetragarn, Y. Laosiritaworn, S. Ananta, R. Yimnirun, Physica Scripta, 77(4), 045702 (2008); https://doi.org/10.1088/0031-8949/77/04/045702